

1 **Anaerobic microbiota facilitate *P. aeruginosa* access to the airway epithelium in a novel co-culture**
2 **model of colonization**

3
4
5 **Patrick J. Moore¹, Talia D. Wiggen¹, Leslie A. Kent¹, Sabrina J. Arif¹, Sarah K. Lucas¹, Scott M.**
6 **O'Grady², Ryan C. Hunter^{1#}**

7
8
9 ¹Department of Microbiology & Immunology, University of Minnesota, 689 23rd Avenue SE, Minneapolis,
10 MN 55455

11 ²Department of Animal Science, University of Minnesota, 1364 Eckles Avenue, Saint Paul, MN 55108
12

13
14 #To whom correspondence should be addressed:

15
16 Ryan C. Hunter
17 Department of Microbiology & Immunology
18 Microbiology Research Facility, 3-115
19 University of Minnesota
20 689 23rd Avenue SE
21 Minneapolis, MN 55455
22 Tel: (612) 625-1402
23 Email: rchunter@umn.edu
24

25
26 **ABSTRACT**

27
28 The role(s) of anaerobic microbiota in chronic airway disease are poorly understood due to inherent
29 limitations of existing laboratory models. To address this knowledge gap, we use a dual oxic-anoxic co-
30 culture approach that maintains an oxygen-limited apical epithelial microenvironment while host cells are
31 oxygenated basolaterally. Reduced oxygen culture did not alter the physiology or gene expression of Calu-
32 3 cells but supported anaerobe-epithelial interactions for 24h without affecting bacterial or host cell viability.
33 Anaerobe challenge led to increased expression of inflammatory marker genes and compromised integrity
34 of apical mucins, leading to our hypothesis that anaerobe-host interactions prime the airways for chronic
35 infection. Indeed, anaerobe pre-treatment of Calu-3 cells led to an increase in *Pseudomonas aeruginosa*
36 colonization. This model system offers new insight into anaerobe-host interactions in airway disease
37 pathophysiology and motivates further study of the lung, gut, and oral cavity, where etiological roles of
38 anaerobes have been proposed but specific pathogenic mechanisms remain unclear.

39 INTRODUCTION

40 Decades of clinical lab culture have focused on a limited set of pathogens associated with acute
41 and chronic airway disease (e.g. *Pseudomonas aeruginosa*, *Staphylococcus aureus*, *Mycobacterium*
42 *tuberculosis*). More recently, culture-independent studies of airway microbiota have identified more
43 complex bacterial signatures, lending evidence to polymicrobial disease etiologies. Notably, oral and
44 supraglottic-associated facultative and obligate anaerobes – *Prevotella*, *Veillonella*, *Streptococcus* spp. –
45 are present at low densities in the healthy respiratory tract (1-4) and are both prevalent and abundant in
46 chronic obstructive pulmonary disease (COPD) (5, 6), cystic fibrosis (CF) (7), non-CF bronchiectasis (8),
47 lung abscess (9), sinusitis (10), idiopathic pulmonary fibrosis (11), and tuberculosis (12). While salivary
48 contamination during sampling remains controversial, consensus is that the development of hypoxic
49 microenvironments within diseased airway mucus provides a niche for anaerobe proliferation, often
50 reaching densities equal to or greater than those of canonical pathogens (7, 13).

51 The function of anaerobic microbiota in airway disease is poorly understood though several roles
52 have been proposed. In healthy individuals, anaerobe abundance in bronchoalveolar lavage fluid
53 correlates with expression of proinflammatory cytokines, elevated Th17 lymphocytes, and a blunted TLR4
54 response, implicating a compromised first line of defense against bacterial infection (1). Indeed,
55 epidemiologic and *in vitro* data suggest that anaerobes may facilitate secondary colonization by canonical
56 airway pathogens. In non-CF bronchiectasis, *Prevotella* and *Veillonella* positively correlate with Th17
57 cytokines and non-tuberculosis mycobacterial infection (14). Similarly, in HIV subjects, anaerobes
58 suppress expression of interferon gamma and IL-17A via production of short-chain fatty acids (SCFAs)
59 and are thought to impair the host response to consequent *M. tuberculosis* colonization (12). In CF,
60 anaerobe-derived SCFAs increase with age and disease progression (15), mediate excessive production
61 of IL-8 by bronchial epithelial cells (in turn promoting neutrophil mobilization) (16) and potentiate the growth
62 and virulence of canonical CF pathogens *in vitro* (17, 18). CF anaerobes have also been reported to
63 increase in abundance during pulmonary exacerbations prior to antibiotic therapy (19), further implicating
64 their role in pathogenesis.

65 While these data collectively support the causality of anaerobic microbiota in airway disease, direct
66 mechanistic studies of anaerobe-host and anaerobe-host-pathogen interactions have been limited by the
67 paucity of compatible laboratory methods. Animal models poorly reflect chronic infection pathologies and
68 are prohibitively expensive for high throughput analyses. As an alternative, the development of three-
69 dimensional (3D) cell cultures have greatly expanded our knowledge of host-microbe interactions at the
70 respiratory epithelial interface (20-22). However, incorporation of anaerobic microbiota into these models
71 is restricted by the inherent challenge of maintaining host cell viability under hypoxic or anoxic culture
72 conditions. New models are needed for a deeper understanding of the role of anaerobic microbiota in acute
73 and chronic airway disease.

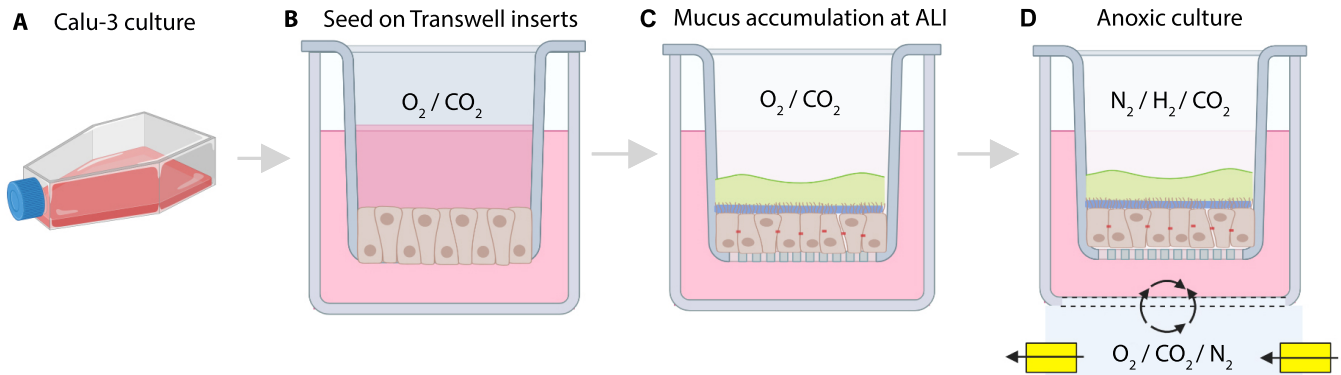
74 A novel system was recently described that enables co-culture of human intestinal enteroids with
75 obligately anaerobic microbiota under reduced oxygen conditions that recapitulate hypoxic
76 microenvironments found *in vivo* (23). Here, we adopted this approach to overcome limitations of studying
77 anaerobe interactions with the airway epithelium in 3D cell culture. First, polarized monolayers of the
78 mucus-overproducing epithelial cell-line, Calu-3, were maintained at air-liquid interface in an anaerobic
79 chamber while O₂ and CO₂ were delivered through a chamber entry port. This setup allows for maintenance
80 of an anoxic microenvironment in the apical compartment while host cells are oxygenated basolaterally.
81 Using this culture system, we establish its utility for the *in vitro* study of anaerobe-airway interactions. We
82 then use this model to test the hypothesis that anaerobic microbiota enhance colonization of the epithelial
83 surface by *P. aeruginosa*. Data presented here not only demonstrate the power and versatility of the anoxic
84 co-culture approach, but also offer new insight into the mechanisms of pathogen colonization and a
85 potential role of anaerobic microbiota in the development of airway infection.

86 **RESULTS**

87 **Optimization and validation of a dual oxic-anoxic airway epithelial culture system.** The primary
88 objective was to establish a cell culture system that facilitates study of anaerobe-host interactions (Figure
89 1). We first cultured polarized monolayers of the adenocarcinoma cell line, Calu-3, at air-liquid interface
90 (ALI) for 21-28 days under standard (normoxic) conditions. As shown previously (24), polarized Calu-3s
91 produce a distinct mucus layer on the apical surface (Figure S1), mimicking aberrant mucin accumulation

92 associated with chronic airway disease. Once polarized, cell cultures were placed in a gas-permeable
93 multi-well plate manifold (Figure S2), transferred to anaerobic chamber, and mixed gas (21% O₂/ 5% CO₂/
94 74% N₂) was delivered through a chamber port to the basolateral compartment of the Transwell-containing
95 plate. Cells were cultured for an additional 24h at anoxic liquid interface (ANLI) prior to analysis.

96



97

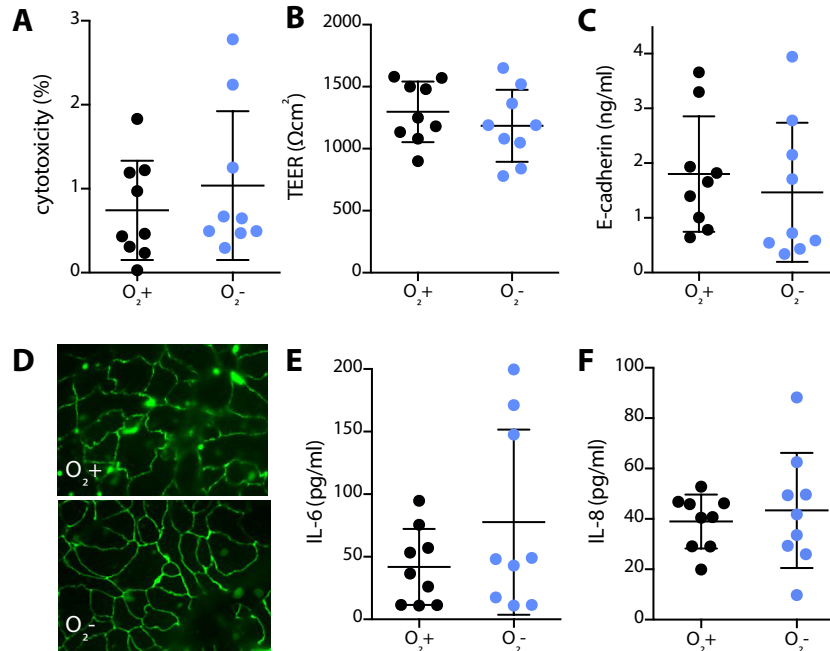
98 **Figure 1. Calu-3 culture at anoxic liquid interface (ANLI).** (A) Calu-3 cells are cultured
99 in MEM with 10% FBS. (B) Cells are seeded on 6.5mm Transwell inserts and grown to
100 confluency (~5 days). (C) Apical medium is removed, and cells are cultured at air-liquid
101 interface (ALI) for 21-28 days prior to (D) incubation under anoxic liquid interface (ANLI)
102 conditions, where the apical compartment is oxygen limited and mixed gas is delivered
103 basolaterally. Figure created with BioRender.com.

104

105 We then determined the effects of ANLI culture, if any, on Calu-3 cell physiology. Quantification of
106 lactate dehydrogenase release showed a negligible increase between normoxic and ANLI culture
107 conditions (p=0.42), suggesting little to no change in viability after 24h (Figure 2A). Transepithelial electrical
108 resistance (TEER) (Figure 2B) and E-cadherin concentrations (Figure 2C), both proxies of epithelial barrier
109 integrity, were also similar between culture conditions (p=0.38 and 0.55, respectively). These data were
110 further supported by immunofluorescence microscopy which revealed confluent monolayers and well-
111 defined staining of the tight junction zonula occludens protein which appeared as near-continuous rings
112 localized to the periphery of each cell (Figure 2D).

113 Previous work has shown hypoxia-induced expression of pro-inflammatory cytokines in primary
114 pulmonary fibroblasts (25). Thus, we used enzyme-linked immunosorbent assays to quantify IL-6 and IL-

115 8 production by Calu-3 cells. Both cytokines showed no significant increases after 24h under ANLI culture
116 conditions relative to normoxic controls (Figure 2E, F, $p=0.21$ and 0.61 , respectively), suggesting that
117 basolateral supply of O_2/CO_2 is sufficient to prevent a pro-inflammatory response.



118

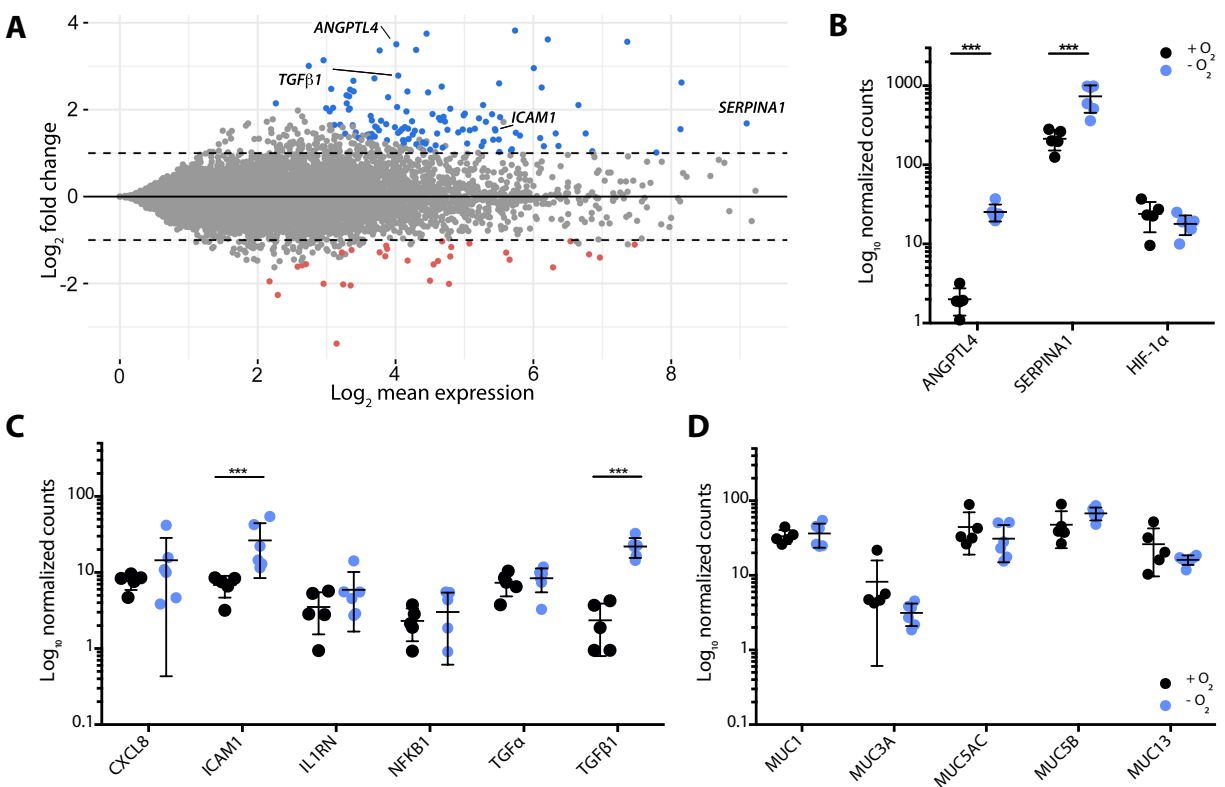
119 **Figure 2. Culture of human bronchial epithelial cells (Calu-3) at ANLI has minimal**
120 **effect on cell physiology. (A)** Cytotoxicity as measured by lactate dehydrogenase (LDH)
121 in the culture medium, **(B)** transepithelial electrical resistance (TEER), **(C)** E-cadherin
122 concentrations, **(D)** immunofluorescence of zonula occludens, and cytokines **(E)** IL-6, and
123 **(F)** IL-8 showed no significant differences between normoxic and ANLI culture conditions.
124 All data shown are for three independent experiments using three biological replicates ($n=9$)
125 and were compared using an unpaired t-test with Welch's correction.

126

127 To gain a broader understanding of the physiological response of Calu-3 cells to ANLI culture, we
128 used RNAseq to compare global Calu-3 gene expression to culture under normoxic conditions.
129 Transcriptome analysis revealed 148 differentially expressed transcripts (117 upregulated, 31
130 downregulated, $l2fc \geq 1$, $padj < 0.001$; out of $\sim 16,000$ total genes) (Figure 3A, Table S1). With the exception
131 of *ANGPTL4* (encoding angiopoietin-like 4) and *SERPINA1* (alpha-1 antitrypsin)(Figure 3B) which are
132 induced in response to hypoxia and acute inflammation, respectively, few markers of cell stress were
133 differentially expressed, including genes involved in tight junction formation, oxidative stress, and
134 endoplasmic reticulum stress. Importantly, HIF-1 α , which is constitutively expressed at low levels under

135 normoxia but upregulated under hypoxia, was also consistent between culture conditions after 24h,
136 suggesting Calu-3 cells were sufficiently oxygenated (Figure 3B). Among inflammatory biomarkers, only
137 *ICAM1* (intracellular adhesion molecule 1) and *TGF β 1* (transforming growth factor beta 1) showed
138 significant differences, further demonstrating that ANLI culture did not yield an appreciably pro-
139 inflammatory microenvironment (Figure 3C). Finally, since we use this model to assay bacterial
140 colonization of the mucus layer, we compared mucin-related gene expression between conditions. Among
141 detectable transcripts (*MUC1*, *MUC3A*, *MUC5AC*, *MUC5B*, and *MUC13*), no significant differences were
142 observed (Figure 3D). These data demonstrate that culture of a respiratory epithelial cell line at anoxic
143 liquid interface yields minimal changes in host cell physiology.

144



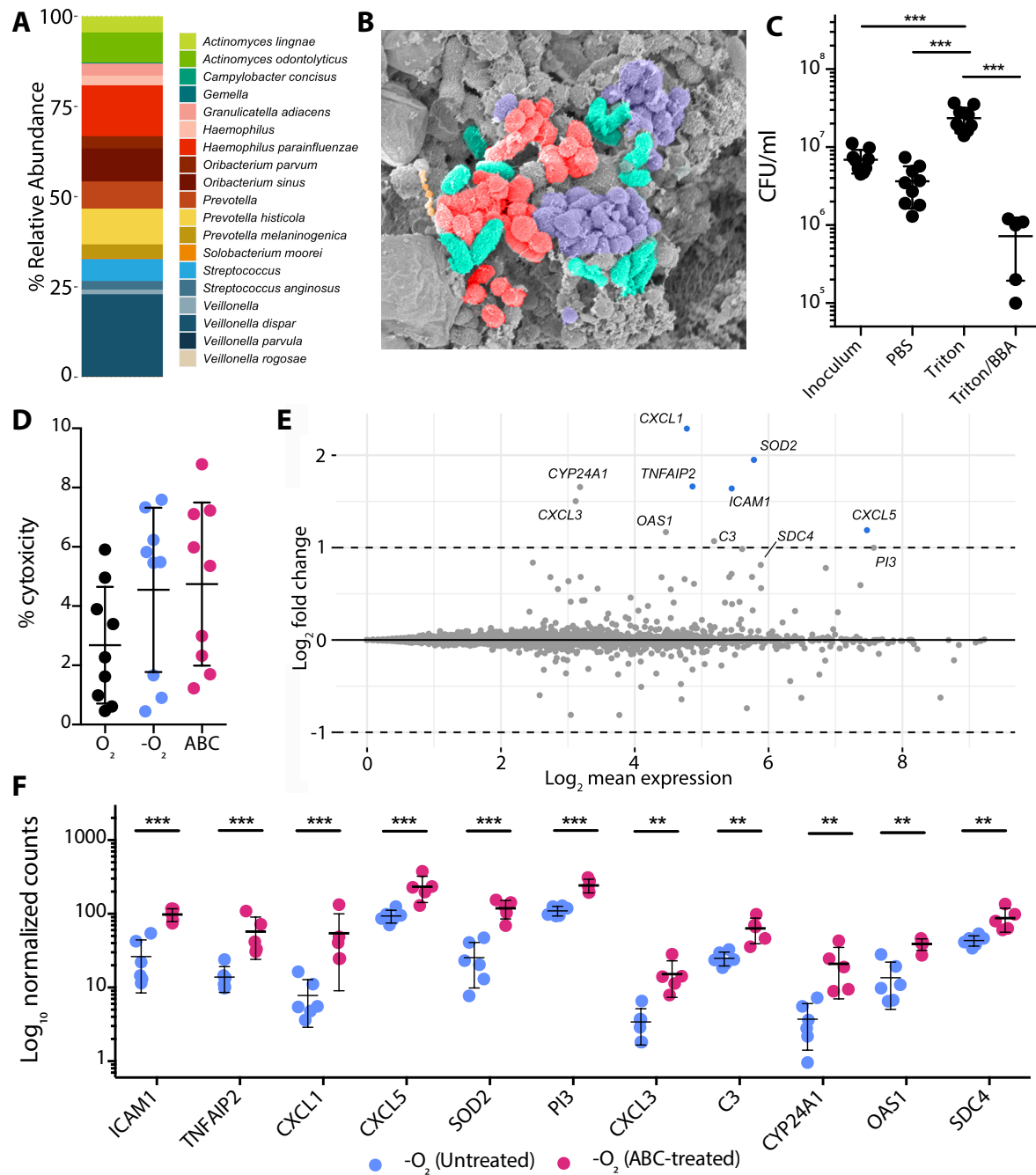
145

146 **Figure 3. Culture of Calu-3 cells at ANLI yields a similar transcriptomic profile to**
147 **normoxic culture conditions (ALI).** (A) MA plot representation of Calu-3 gene expression at
148 ANLI relative to normoxic culture (ALI). (B) *ANGPTL4* and *SERPINA1* were differentially
149 expressed, though HIF-1 α was consistent between cultures. Few changes in (C) inflammatory
150 biomarkers and (D) mucin gene expression were observed. Data shown in panels B-D are
151 log₁₀-normalized gene counts from five or six independent biological replicates and were
152 compared using the Wald test, Benjamini-Hochberg adjusted (***, p<0.001).

153 **Anaerobic airway microbiota induce an inflammatory host response.** To date, the lack of tractable
154 cell culture systems compatible with hypoxic or anoxic growth has limited our understanding of host-
155 anaerobe interactions. Prior work has shown that culture supernatants of anaerobic bacteria elicit pro-
156 inflammatory cytokine expression *in vitro* through mixed-acid fermentation and production of SCFAs (1,
157 15, 16). However, it is not yet known how the host responds to the physical presence of anaerobes at the
158 airway epithelial interface. To address this knowledge gap, we used our ANLI culture approach to assess
159 the response of Calu-3 cells to co-culture with anaerobic microbiota.

160 As a starting point, we used a defined anaerobic bacterial consortium (ABC) enriched from airway
161 mucus derived from an individual with chronic sinusitis. This representative community was chosen for its
162 dominant bacterial taxa (*Veillonella*, *Prevotella*, *Streptococcus*) associated with both healthy and diseased
163 airways (Figure 4A). These genera are also known for their mucin-degradation capacity and the ability to
164 support pathogen growth through nutrient cross-feeding (17). After 3h of equilibration at ANLI, Calu-3 cells
165 were apically challenged with the anaerobic consortium ($\sim 8 \times 10^6$ CFUs) and incubated for an additional
166 24h. Colonization was confirmed using scanning electron microscopy which revealed bacterial cells at the
167 epithelial interface (Figure 4B). Importantly, anaerobes (4×10^6 CFUs) were recovered after 24h by
168 washing with PBS and plating on Brain Heart Infusion agar (BHI), while washing with Triton X-100 resulted
169 in a 0.7-log increase in recovery (1.6×10^7 CFUs), suggesting both anaerobe growth at the epithelial
170 surface and either robust attachment or bacterial invasion of host cells (i.e., cells were not removed by
171 PBS washing alone). Recovery of $\sim 7 \times 10^5$ CFUs on a *Prevotella*-selective medium (Brucella Blood Agar,
172 BBA) confirms that apical oxygen concentrations were sufficiently reduced to facilitate strict anaerobe
173 growth. Despite this growth, cytotoxicity was not induced by anaerobe challenge after 24h (Figure 4D).

174 We then used RNAseq to profile the Calu-3 transcriptional response to anaerobe (ABC) challenge
175 (Figure 4E, Table S2). Contrary to our expectation, only five genes were differentially expressed relative
176 to untreated ANLI cell cultures (all upregulated, $l2fc \geq 1$, $p_{adj} < 0.001$), though all were markers of
177 inflammation. These included *ICAM1*, *TNFAIP2* (mediated by $TNF\alpha$ in response to bacterial challenge)
178 (26), chemokines *CXCL1* and *CXCL5* (neutrophil chemoattractants primarily expressed as an acute



179

180

181

182

183

184

185

186

187

188

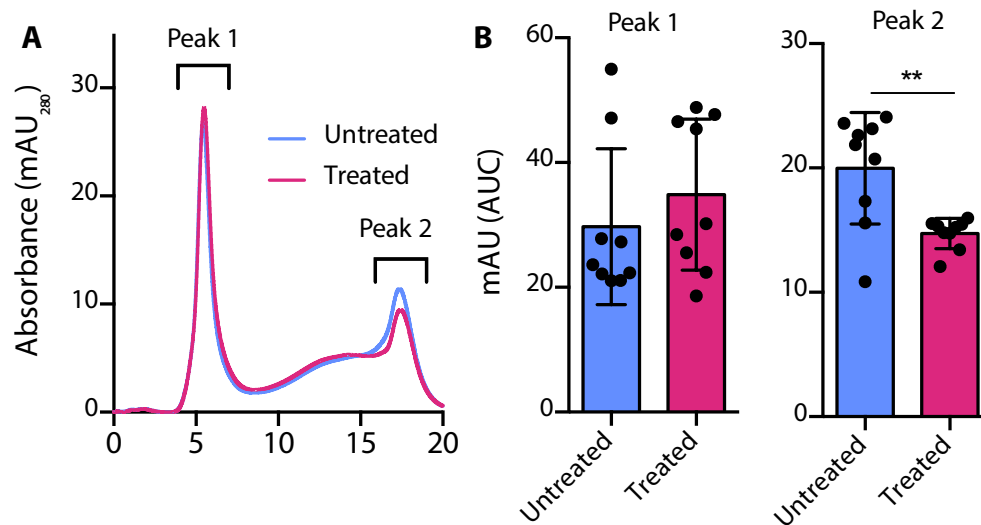
189

Figure 4. Anaerobic microbiota colonize the apical surface of Calu-3 cells and induce a pro-inflammatory response. (A) Taxonomic composition of an anaerobic bacterial consortium (ABC) derived from the upper airways. (B) SEM micrograph of Calu-3 cells after CRS challenge. (C) Bacterial recovery from Calu-3 cells after 24h by washing with PBS, TritonX-100, and plating on *Prevotella* selective agar (BBA). (D) Anaerobe (ABC) challenge did not result in Calu-3 cytotoxicity relative to unchallenged cells. (E) MA plot representation of Calu-3 gene expression under ANLI after ABC challenge relative to an untreated ANLI control. (F) Log₁₀-normalized gene counts from five or six independent biological replicates. Data in panels C and D were compared using a one-way ANOVA ($p < 0.0001$) with multiple comparisons test. Data in panels E and F were compared using a Wald test, Benjamini-Hochberg adjusted ($***p < 0.001$, $**p < 0.01$).

190 inflammatory response to infection) (27, 28), and *SOD2* (superoxide dismutase 2, expressed in response
191 to bacterial LPS and has an antiapoptotic role against inflammatory cytokines) (29). Other inflammatory
192 markers including *PI3* (elafin, an elastase inhibitor that can prime innate immune responses in the lung)
193 (30), *CXCL3*, *C3* (complement), *CYP24A1* (cytochrome p450 family 24 subfamily A member 1), *OAS1*
194 (oligoadenylate synthetase), and *SDC4* (syndecan 4) were also differentially expressed, though did not
195 reach our threshold p_{adj} of <0.001 (Figure 4F).

196

197 **Anaerobic microbiota alter the mucosal interface through mucin degradation.** Our previous work
198 demonstrated the functional capacity of anaerobic microbiota to degrade airway mucins and support the
199 growth of canonical pathogens via nutrient cross-feeding (17). Thus, in support of downstream pathogen
200 colonization experiments, we used fast protein liquid chromatography (FPLC) to determine whether
201 anaerobe challenge altered Calu-3 mucin integrity relative to unchallenged cells. To do so, we collected
202 and purified mucin from the apical side of the Transwells as previously described (24) and used CL-4B
203 size-exclusion chromatography to assay their integrity. As expected, chromatograms revealed two
204 characteristic peaks; (i) high molecular weight mucins which ran in the void volume of the column, and (ii)
205 a broader inclusion volume peak representative of lower molecular weight mucins (31, 32) (Figure 5A).
206 While differences in the chromatographic profile of peak 1 (high molecular weight mucins) were negligible
207 between culture conditions ($p=0.38$), peak 2 area was significantly reduced ($p=.007$) following anaerobe
208 challenge (Figure 5B), reflecting degradation of lower-molecular weight mucin glycoproteins. Together,
209 these data suggest that in addition to eliciting a pro-inflammatory host response, anaerobic colonization
210 alters the physicochemical properties of mucosal interface.



211

212

213

214

215

216

217

218

219

Figure 5. Anaerobic microbiota alter epithelial mucin integrity. (A) Representative FPLC traces of MUC5AC mucins purified from Calu-3 cells grown at ANLI (untreated) and after treatment with an anaerobic bacterial community (ABC, treated). (B) Area under curve (AUC) for both peak 1 (high molecular weight mucins) and peak 2 (low molecular weight mucin). Data shown were derived from three independent experiments using three biological replicates (n=9). Data were compared using a unpaired t-test with Welch's correction (**, p<.01).

219

220 **Anaerobes promote *P. aeruginosa* colonization of the airway epithelium.** Recent work has shown
221 that viral challenge of the respiratory epithelium potentiates colonization by *P. aeruginosa* via interferon
222 mediated effects (20). Other work has shown that the protective role of the mucus barrier is compromised
223 by *Streptococcus mitis* through hydrolysis of mucin glycans (33). Given that the anaerobes used in our
224 model both elicited an inflammatory response and altered mucin integrity, we hypothesized that in addition
225 to providing nutrients for pathogen growth through cross-feeding (17), anaerobic microbiota enhance *P.*
226 *aeruginosa* colonization of the airway epithelium (depicted in Figure 6A).

227

228

229

230

231

To test this hypothesis, Calu-3 cells were first treated with the anaerobic bacterial consortium (ABC)
for 24h, washed to remove spent medium and unbound cells, and subsequently infected with 1×10^6 CFUs
of *P. aeruginosa* PA14 for 2h. Removal of spent medium and a short incubation time ensures that any
difference in colonization between anaerobe-treated cells and an unconditioned (i.e., no anaerobe) control
was a result of cell attachment and not enhanced growth. *P. aeruginosa* colonization was then determined

232 by washing and permeabilization of Calu-3 cells followed by plate enumeration. As predicted, anaerobe
233 pre-treatment resulted in an increase in 1.1×10^7 *P. aeruginosa* CFUs relative to untreated (i.e., no ABC)
234 controls ($p=0.0003$, Figure 6B).

235 To further demonstrate that enhanced pathogen colonization was due to mucin degradation and
236 not some other unidentified process, mucins isolated from Calu-3 cells treated with ABC (and untreated
237 controls) were used to coat the surface of a microtiter plate (34), followed by addition of *P. aeruginosa*
238 PA14. As expected (35), mucin coating led to a 1.5 log-reduction in bacterial attachment relative to
239 uncoated plates (PBS alone). Consistent with our ANLI co-culture assay, ABC-treated mucins resulted in
240 a significant increase ($p=0.0007$) in *P. aeruginosa* binding compared to untreated mucins (Figure 6C). To
241 confirm that our mucin purification process (e.g., use of guanidine hydrochloride) did not affect *P.*
242 *aeruginosa* viability, plates were also coated with mucins degraded with human neutrophil elastase (NE)
243 and isolated using the same process. NE-treated mucins resulted in similar PA14 attachment to PBS
244 controls, confirming bacterial viability and that anaerobe-microbiota can enhance pathogen colonization of
245 a mucin-coated interface.

246 Finally, to assess the contributions of individual anaerobes to *P. aeruginosa* colonization we
247 challenged Calu-3 cells with representative isolates of the three most abundant genera in the anaerobic
248 consortium (*Streptococcus*, *Veillonella*, *Prevotella*) prior to *P. aeruginosa* colonization (Figure 6D).
249 Contrary to a recent study (33), we found that *Streptococcus* species (*S. gordonii* and *S. parasanguinis*)
250 had little effect on PA14 colonization, despite their known mucin degradation capacity. Similarly, *V. parvula*
251 resulted in no significant differences between treatment conditions. By contrast, challenge with both *P.*
252 *melaninogenica* and *P. oris*, two species commonly associated with inflammatory airway disease, resulted
253 in significantly increased PA14 recovery from Calu-3 cells compared to unconditioned controls ($p=0.0003$
254 and $p=0.0004$, respectively). These data demonstrate that while anaerobic microbiota of the respiratory
255 tract likely facilitate enhanced colonization of the airway epithelium via mucin degradation, it is clear they
256 do so in a species-specific manner.

257

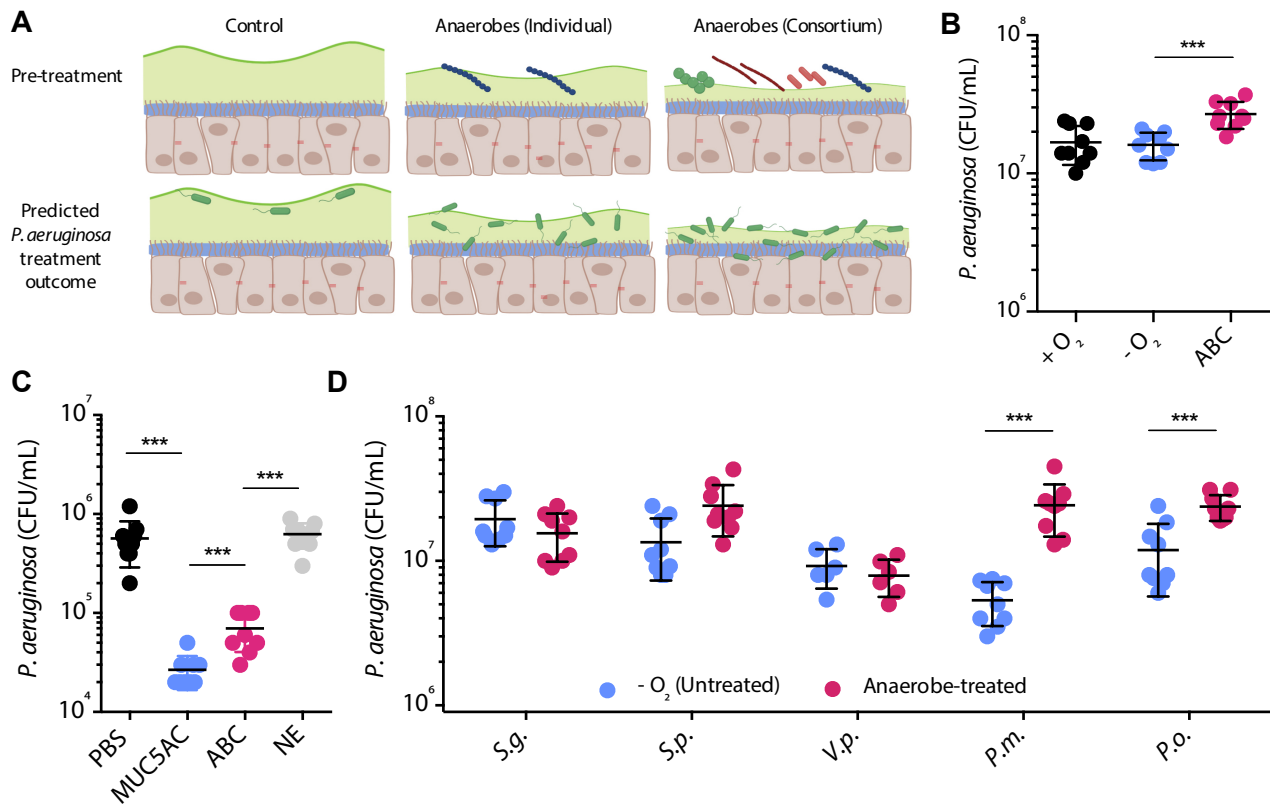


Fig. 6. Anaerobic microbiota condition the epithelial interface for pathogen colonization. (A) Schematic of experimental design. (B) Calu-3 pre-treatment with an anaerobic bacterial consortium (ABC) potentiates *P. aeruginosa* colonization. (C) *P. aeruginosa* adhesion to microtiter plates coated with mucin (MUC5AC), ABC-treated mucin, and neutrophil elastase (NE)-treated mucin relative to an uncoated control (PBS). (D) *P. aeruginosa* adhesion to Calu-3 cells after pre-treatment with individual anaerobes (*S.g.*, *Streptococcus gordonii*; *S.p.*, *S. parasanguinis*; *V.p.*, *Veillonella parvula*; *P.o.*, *Prevotella oris*; *P.m.*, *P. melaninogenica*). Data shown in panels B-D were derived from three independent experiments with three biological replicates (n=9). Data in C were compared using a one-way ANOVA ($p < 0.0001$) with multiple comparisons. Data in C were compared using a non-parametric Kruskal-Wallis test ($p < 0.0001$) with multiple comparisons. Pairwise comparisons in panel D were performed using an unpaired t-test with Welch's correction ($*p < 0.05$, $***p < 0.001$).

258

259

260

261

262

263

264

265

266

267

268

269

270

271

272 DISCUSSION

273

274

275

276

277

278

The recent surge in culture-independent sequencing of human microbiota has spawned renewed interest in the importance of anaerobic bacteria in disease etiologies. However, despite anaerobes comprising a significant component of airway bacterial communities, studies on their contributions to disease pathophysiology have reported seemingly contradictory results (7, 19, 36-41), calling into question their role in patient morbidity. Proposed pathogenic mechanisms are supported by compelling *in vitro* data (15-17, 42, 43), but their relevance is unresolved due to a lack of compatible models with which to test

279 their interactions with the respiratory epithelium. To address this knowledge gap, here we optimized and
280 characterized a model system that facilitates co-culture of anaerobes and polarized airway epithelial cells.
281 Importantly, provision of oxygen exclusively to the basolateral side of host (Calu-3) cells prevented anoxia-
282 associated cytotoxicity, inflammation, and significant changes in global gene expression over 24h,
283 validating its utility for the extended study of anaerobe-host interactions. Using this model, we demonstrate
284 that anaerobic microbiota stimulate an immune response and promote enhanced epithelial colonization by
285 airway pathogens.

286 Disparate oxygen demands of epithelial cells and anaerobic bacteria pose significant challenges
287 for their co-culture *in vitro*. Several bacterial-epithelial culture systems have been developed in an attempt
288 to overcome these challenges and recapitulate an oxygen-restricted mucosal interface (44-47), though
289 each has notable drawbacks. Transwell cultures of Caco-2, HaCaT, and primary human gingival cells have
290 been used to demonstrate that anaerobic taxa can adhere to, invade, and alter oral and intestinal epithelia,
291 yet these assays are either limited to short incubation times or poorly mimic atmospheric conditions
292 observed *in vivo* (48-51). Newer microfluidic-based and ‘organ-on-a-chip’ models have also seen
293 widespread interest due to their ability to establish dual oxic-anoxic interfaces and facilitate study of
294 anaerobe-host interactions (52-56). However, these models either preclude direct host-bacterial contact
295 or are technically challenging to maintain both oxic and strict anoxic microcompartments. More recently,
296 new methods have been expanded to include respiratory epithelial cells and used to study alveolar cell
297 infection by *M. tuberculosis*, but development is still in its infancy (57). Our adapted system offers the
298 distinct advantages of ease-of-use, direct interactions between host and microbiota, reproducibility given
299 the multi-well plate format, and methodological flexibility lending itself to genetic, biochemical, and
300 microscopy studies as demonstrated here. Most notably, this co-culture model elicits few changes in host
301 cell physiology after 24h of anoxia, paving the way for a greater understanding of the mechanistic
302 contributions of anaerobic bacteria to airway pathophysiology.

303 To demonstrate the utility of our model we used a polymicrobial consortium representative of
304 anaerobic bacterial community signatures observed in acute and chronic airway disease (8, 11, 39, 58).
305 Dominated by *Streptococcus*, *Prevotella*, and *Veillonella* spp., this consortium (among other bacterial taxa)

306 is thought to seed the airways through microaspiration from the oral cavity and is recognized as a key risk
307 factor in the development of COPD, CF, pneumonia, sinusitis and other diseases. For example, *in vitro*
308 studies have shown that anaerobe-derived supernatants containing proteases and pro-inflammatory short-
309 chain fatty acids modulate the immune tone of bronchial epithelial cell lines and primary cell cultures (15,
310 16). Indeed, anaerobe abundance in both diseased airways and healthy controls is associated with
311 enhanced expression of inflammatory cytokines (1, 12). Our data also support a immunomodulatory role
312 and suggest that colonization of the airway mucosa by aspirated anaerobes may establish a local
313 inflammatory environment known to promote colonization by *P. aeruginosa* and other canonical pathogens
314 (20, 21).

315 We previously reported that anaerobes can also stimulate pathogen growth through mucin-based
316 cross-feeding (17). Specifically, *P. aeruginosa*, which cannot efficiently catabolize mucins in isolation, can
317 gain access to bioavailable substrates via anaerobe-mediated degradation of the mucin polypeptide and
318 O-linked glycans. Though not directly tested here, it is plausible that pre-colonization with an anaerobic
319 bacterial community liberates additional mucin-derived metabolites on which pathogens can thrive at the
320 epithelial interface. While it remains unclear why only low molecular weight mucins were altered, our FPLC
321 data confirm that the mucosal surface is structurally modified as a result of anaerobic colonization. Given
322 that mucin degradation has been shown to compromise its barrier function and enhance pathogen-
323 epithelial interactions (33), we propose that in addition to the host's impaired mucociliary clearance,
324 pathogenic contributions of anaerobic microbiota to airway infection are likely imparted through a
325 multifactorial process (inflammation, cross-feeding, and surface alteration).

326 By focusing on an early time point after *P. aeruginosa* challenge (2h), we targeted anaerobic mucin
327 degradation and its role in re-shaping the epithelial interface while enhancing pathogen attachment, as
328 was previously shown for *S. mitis* and *Neisseria meningitidis* (33). As predicted, anaerobe degradation of
329 apical mucus resulted in a significant increase in *P. aeruginosa* attachment, which has important clinical
330 implications. Most notably, epithelial colonization is known to stimulate rapid *P. aeruginosa* biofilm
331 maturation and associated increases in extracellular polysaccharide production, induction of quorum-
332 sensing and other transcriptional changes (22). In addition, *P. aeruginosa* grown on bronchial epithelial

333 cells is far more resistant to antibiotic treatment than when grown on abiotic surfaces (22), consistent with
334 their increased tolerance *in vivo*. We propose that anaerobe-mediated colonization further potentiates
335 these phenotypes. Moving forward, it will be important to consider *P. aeruginosa* interactions with the host
336 over longer time periods to further understand differences in pathogen physiology and the inflammatory
337 host response in the presence and absence of anaerobic microbiota.

338 We elected to use Calu-3 cells as a representative cell line for several reasons. First, Calu-3 cells
339 reach polarization at ALI within ~21 days, express high levels of occludin and E-cadherin localized at tight
340 junctions, and achieve TEER values ($>1000 \Omega\text{cm}^2$) far greater and more stable than those of primary cells
341 (59-61). In addition, Calu-3s express high levels of CFTR (62), demonstrating their suitability and relevance
342 for studies of CF and COPD, for which CFTR-silencing small hairpin RNAs (shRNA) have already been
343 developed (63). Finally, unlike many other respiratory cell lineages, overproduction of mucus on the apical
344 surface of polarized Calu-3 cells mimics a diseased mucosal environment and allowed us to test the
345 hypothesis that mucin degradation enhances pathogen colonization. This was an important consideration
346 as *P. aeruginosa* biofilms, at least in the context of CF, are thought to form within secreted mucus as
347 opposed to the epithelial layer (64, 65). We also acknowledge limitations. Unlike primary cells, which form
348 a pseudostratified epithelium with mucociliary differentiation, Calu-3 cells are derived from human
349 bronchial submucosal glands that comprise a relatively homogenous monolayer. Transcriptional and
350 physiological responses to external stimuli may also be unique to Calu-3s. As an example, *S. aureus*
351 enterotoxin B is known to elicit significant differences in barrier integrity, IL-6 and IL-8 production relative
352 to primary tissue (66). These, among other distinctions, underscore the importance of future work testing
353 additional cell lines and primary tissue.

354 Despite these limitations, our model represents a tractable co-culture system that facilitates
355 extended interrogation of host-anaerobe interactions. While we use this model here to demonstrate a role
356 for anaerobic microbiota in the initial colonization of the epithelial surface, this work will undoubtedly benefit
357 future studies focused on anaerobe-host and anaerobe-host-pathogen interactions and their dynamics
358 over time. Not only do we anticipate generating a deeper understanding of *P. aeruginosa* pathophysiology
359 under oxygen-limited conditions, we also expect to identify new therapeutic strategies in addition to

360 understanding how existing antimicrobials are impacted by environmental conditions known to exist *in vivo*
361 (64). Finally, while we use an airway-derived bacterial community and *P. aeruginosa* as our model
362 organisms, this work motivates additional studies of the gut, lung, oral cavity, and other sites of infection,
363 where etiological roles of anaerobes have been proposed but specific pathogenic mechanisms remain
364 unclear.

365

366 **METHODS**

367 **Epithelial Cell Culture.** Calu-3 cells were maintained in Minimal Essential Medium (Corning, USA) in 10%
368 fetal bovine serum (FBS, Gene) supplemented with 100 U/mL penicillin and 100 µg/mL streptomycin
369 (Gibco) at 37°C in a 5% CO₂ incubator. Upon reaching 80% confluency, 1 x 10⁵ cells were passaged onto
370 6.5mm culture inserts (12-well hanging inserts, 0.4 µm pore; Corning). When cells reached confluency (~5
371 days), apical medium was removed to establish an air-liquid interface (ALI). Polarized cells were
372 maintained for an additional 21-28 days to facilitate differentiation and mucus accumulation.

373 Cell cultures were then assembled in a gas permeable multi-well plate manifold based on an
374 enteroid-anaerobe co-culture system recently described (23) (Figure S2). Briefly, once polarized, Calu-3
375 cells were placed into gaskets in a 24-well gas-permeable plate (CoyLabs, Grass Lake, MI) containing
376 800µl of MEM per well. Mineral oil (400µL) was added to unused wells to prevent gas permeation from the
377 basolateral to apical side of the manifold. Once assembled, the apparatus was moved to an anaerobic
378 chamber (90% N₂/5% H₂/5% CO₂) while mixed gas (21% O₂/5% CO₂/74% N₂) was delivered to the base
379 of the plate to oxygenate the basolateral side of the polarized monolayer. A schematic of this workflow is
380 summarized in Figure 1.

381 **Cell culture assays.** Calu-3 barrier integrity was determined by trans-epithelial electrical resistance
382 (TEER) measured with a Millicell-ERS2 Volt-Ohm meter (Millipore Sigma). Barrier integrity was further
383 assessed using the Human E-cadherin Quantikine enzyme-linked immunosorbent assay (ELISA) kit (R&D
384 Systems, Minneapolis, MN). Absorbance was measured at 450 nm using a BioTek Synergy H2 plate
385 reader and concentrations of E-cadherin were determined against a standard curve according to

386 manufacturer's instructions. Tight junction formation was assayed using immunofluorescence with an anti-
387 zona occludens (ZO)-1 monoclonal antibody (Thermo). To do so, Calu-3 cultures on Transwell inserts
388 were chemically fixed in 4% paraformaldehyde (PFA) in phosphate-buffered saline (PBS) for 1h at room
389 temperature. Cells were blocked in 10% goat serum and 1% bovine serum albumin (Sigma) for 15 min.
390 After blocking, cells were incubated with human anti-mouse ZO-1 (AlexaFluor-488 conjugate;
391 ThermoFisher)(5 μ g/mL) for 1h. Transwell membranes were washed, removed from the supporting plastic
392 insert, and mounted on glass slides using Vectashield anti-fade mounting medium. Labeled cells were
393 visualized (ex. 480nm, em. 525nm) on an Olympus IX83 inverted fluorescence microscope using a 20X
394 objective lens (0.75 NA). Finally, cytotoxicity was determined by lactate dehydrogenase measurements on
395 cell-free supernatants using the Cytotoxicity Detection Kit Plus assay (Roche) according to manufacturer's
396 instructions. Data were calculated as percent LDH release compared with a lysed control and reported as
397 %LDH release = [(experimental value low control)/(high control-low control)] x 100.

398 **Immunoassays.** The pro-inflammatory cytokine response of Calu-3 cells was measured after 24h of
399 culture in the anaerobic chamber. To do so, spent medium was collected from the apical side of Transwell
400 cultures, and tumor necrosis factor alpha (TNF- α), interleukin (IL-) 8 and IL-6 were then measured by
401 ELISA per manufacturer instructions (R&D systems). Cells grown under standard incubator conditions (5%
402 CO₂) were used as a control.

403 **FPLC.** Secreted mucins were collected from Calu-3 cells as previously described (24). Briefly, cells grown
404 on Transwell inserts were solubilized in a reduction buffer consisting of 6M guanidine hydrochloride, 0.1M
405 Tris-HCl buffer, and 5mM EDTA (pH 8). Prior to solubilization, 10mM dithiothreitol (DTT) and a cComplete
406 Mini protease inhibitor tablet (Roche) were added to 400mL of reduction buffer to minimize mucin
407 degradation. Cell suspensions were gently agitated by pipetting to dislodge biomass, and each of the six
408 Transwell suspensions per plate were pooled into a single aliquot. Cells were rinsed with a reduction buffer
409 to remove residual mucin. This mixture was then incubated for 5h at 37°C, followed by the addition of 25
410 mM iodoacetamide and incubation overnight at room temperature. Mucins were then dialyzed (1000 kDa
411

412 MWCO) against 1L of 4M GuHCl buffer containing 2.25 mM NaH₂PO₄-H₂O and 76.8 mM Na₂HPO₄ and
413 proceeded for 36h with buffer exchanges every 12h.

414 Fast protein liquid chromatography (FPLC) size-exclusion chromatography was then used to
415 evaluate the integrity of high-molecular weight mucins. Using an Akta Pure FPLC (GE Healthcare
416 BioSciences, Marlborough, MA) housed at 4°C, 500 µL of purified mucin was manually injected and
417 subjected to an isocratic run at a flow rate of 0.4 mL/min for 1.5 column volumes (CV) with 150mM NaCl
418 in 50 mM phosphate buffer (pH 7.2) on a 15mL 10/200 Tricorn column packed with Sepharose 4B-CL
419 beads. Data were collected using Unicorn 7 software (GE Healthcare Biosciences).

420 **Bacterial strains and culture conditions.** *P. aeruginosa* PA14 was obtained from D.K. Newman
421 (California Institute of Technology) and was routinely cultured on Luria Bertani (LB) medium. *P.*
422 *melaninogenica* ATCC 25845, *S. parasanguinis* ATCC15912, and *V. parvula* ATCC10790 were obtained
423 from Microbiologics (St. Cloud, MN). *S. gordonii* was obtained from M.C. Herzberg (University of
424 Minnesota) and *P. oris* 12252T was purchased from the Japan Collection of Microorganisms. All anaerobes
425 were maintained on Brain-Heart Infusion medium supplemented with hemin (0.25 g/L), vitamin K (0.025
426 g/L) and laked sheep's blood (5% vol/vol) (BHI-HKB) in an anaerobic chamber. A mucin-enriched
427 anaerobic bacterial community (ABC) derived from an individual with chronic rhinosinusitis was also used
428 and was cultured in a minimal mucin medium (MMM) described previously (17).

429 **Bacterial challenge and infection.** Forty-eight hours prior to bacterial challenge, Calu-3 cells were
430 incubated in MEM/FBS without antibiotics. On the day of bacterial challenge, Transwells were assembled
431 in the gas permeable culture system and transferred into the anaerobic chamber where they were allowed
432 to equilibrate for 3h. Overnight cultures of each anaerobe and the anaerobic community (ABC) were grown
433 in MMM. Each individual culture was diluted to a concentration of ~1 x 10⁶ colony forming units (CFU) in
434 MEM and 10 µL of bacterial suspension was added to the apical side of the Calu-3 cells. Similarly, 10 µL
435 of an adjusted suspension (OD_{600nm} = 0.1) of the anaerobic community was added to separate wells.
436 Co-cultures were then incubated for an additional 24h. Following anaerobe challenge, spent medium was
437 collected and analyzed for cytotoxicity using the LDH colorimetric assay (described above). Mucins were

438 also collected as described above for integrity analysis via FPLC. In a separate experiment, anaerobe
439 viability was determined using plate enumeration. Briefly, Calu-3 cells were washed with 100 μ L of PBS (to
440 remove loosely bound cells) or 0.25% Triton X-100 (to recover tightly bound or intracellular bacteria).
441 Resulting washes were serially diluted and plated on BHI or Brucella Laked Blood Agar (BBA) with
442 Kanamycin (100 μ g/mL) and Vancomycin (7.5 μ g/mL) for enumeration.

443 For the *P. aeruginosa* colonization assay, Calu-3 cultures were removed from the anaerobic
444 chamber following anaerobe challenge. Cells were gently washed with PBS and subsequently infected
445 with 1×10^6 CFU of *P. aeruginosa* for 2h. After incubation, cells were gently washed three times with PBS
446 to remove unbound *P. aeruginosa* and were permeabilized using 0.25% Triton X-100. Bacteria were
447 enumerated by plating serial dilutions of Calu-3 cell lysates on LB agar. All assays were performed using
448 three biological replicates and data are reported as the mean of three experiments.

449 **RNA sequencing.** The transcriptomic response of Calu-3 cells to anoxic culture and anaerobe challenge
450 was determined using RNAseq. Calu-3 cells were cultured at ALI as described above and harvested after
451 24h of anaerobic incubation in the presence/absence of bacterial challenge. Normoxic (unchallenged) cells
452 were maintained under standard incubator conditions. At the conclusion of each experiment, RNAlater
453 (Invitrogen) was added to the apical and basolateral side of each well. For each condition, RNA was
454 isolated from 5 or 6 Transwells using the RNeasy Micro Plus kit (Qiagen) according to manufacturer's
455 instructions. DNase treatment was performed as part of the RNA Clean and Concentrator kit (Zymo). RNA
456 quality (RIN > 9.7) and quantity were assessed using an Agilent Bioanalyzer and RiboGreen, respectively.
457 cDNA libraries were prepared using the SMARTer Universal Low Input RNA Kit (Takara Bio) and submitted
458 for sequencing at the University of Minnesota Genomics Center on the Illumina NovaSeq 6000 platform.
459 The Ensembl GTF annotation file was filtered to remove annotations for non-protein-coding features.
460 Fastq files were evenly subsampled down to a maximum of 100,000 reads per sample. Data quality in
461 fastq files was assessed with FastQC. Raw reads were mapped to reference Human (Homo_sapiens)
462 genome assembly "GRCh38" using annotation from Ensembl release 98. Gene counts were generated
463 with 'featureCounts' of the RSubread package (67). DESeq2/1.28.1 was used to estimate size factors to

464 generate normalized count data, estimate gene-wise dispersions, shrink estimates using `type='ashr'`, and
465 perform Wald hypothesis testing (68, 69). Genes with a \log_2 fold-change greater than 1 and Benjamini-
466 Hochberg adjusted p-value < 0.001 were considered significant. Code and data files are shared at
467 [https://github.com/Hunter-Lab-UMN/Moore PJ 2020](https://github.com/Hunter-Lab-UMN/Moore_PJ_2020).

468 **Scanning electron microscopy.** Untreated, anaerobe-challenged, and *P. aeruginosa*-infected cell
469 cultures were washed three times in 0.2M sodium cacodylate buffer, and submerged in primary fixative
470 (0.15 M sodium cacodylate buffer, pH 7.4, 2% paraformaldehyde, 2% glutaraldehyde, 4% sucrose, 0.15%
471 alcian blue 8GX) for 22h. Transwell membranes were washed three more times prior to a 90 minute
472 treatment with secondary fixative (1% osmium tetroxide, 1.5% potassium ferrocyanide, 0.135M sodium
473 cacodylate, pH 7.4). After three final washes, cells were dehydrated in a graded ethanol series (25%, 50%,
474 75%, 85%, 2 x 95%, and 2 x 100%) for 10 minutes each before CO₂-based critical point drying. Transwell
475 membranes were attached to SEM specimen mounts using carbon conductive adhesive tape and sputter
476 coated with ~5 nm iridium using the Leica ACE 600 magnetron-based system. Cells were imaged using a
477 Hitachi S-4700 field emission SEM with an operating voltage of 2kV. Images were false colored using
478 Adobe Photoshop CS6.

479 **Microtiter plate binding assay.** *P. aeruginosa* adhesion to mucus was tested using an established
480 microtiter plate-based assay (34). 96 well MaxiSorp microtiter plates (Nunc) were coated with 40 μ g/ml of
481 mucins (MUC5AC) derived from untreated and ABC-treated Calu-3 cells. As a control, MUC5AC treated
482 with neutrophil elastase (1 μ g/mL) was also used. After coating, plates were incubated for 24h at 37°C.
483 Mucin-coated wells were then washed three times with sterile PBS to remove any residual unbound mucin.
484 1×10^6 CFUs of *P. aeruginosa* PA14 were added to mucin-coated wells and incubated for an additional 2h
485 at 37°C. Wells were washed 10 times with PBS to remove any unbound bacteria. Bound PA14 was
486 desorbed by treatment with 200 μ l of 0.25% Triton X-100 for 15 min at room temperature. Bacteria bound
487 to each well were enumerated by plating serial dilutions on LB agar. All assays were performed using three
488 biological replicates and data are reported as the mean of three experiments (n=9).

489 **REFERENCES**

- 490 1. L. N. Segal, A. V. Alekseyenko, J. C. Clemente, R. Kulkarni, B. Wu, Z. Gao, H. Chen, K. I. Berger, R.
491 M. Goldring, W. N. Rom, M. J. Blaser, M. D. Weiden, Enrichment of lung microbiome with supraglottic
492 taxa is associated with increased pulmonary inflammation. *Microbiome* **1**, 19 (2013).
- 493 2. E. S. Charlson, K. Bittinger, A. R. Haas, A. S. Fitzgerald, I. Frank, A. Yadav, F. D. Bushman, R. G.
494 Collman, Topographical continuity of bacterial populations in the healthy human respiratory tract. *Am*
495 *J Respir Crit Care Med* **184**, 957-963 (2011).
- 496 3. A. Morris, J. M. Beck, P. D. Schloss, T. B. Campbell, K. Crothers, J. L. Curtis, S. C. Flores, A. P.
497 Fontenot, E. Ghedin, L. Huang, K. Jablonski, E. Kleerup, S. V. Lynch, E. Sodergren, H. Twigg, V. B.
498 Young, C. M. Bassis, A. Venkataraman, T. M. Schmidt, G. M. Weinstock, L. H. M. Project, Comparison
499 of the respiratory microbiome in healthy nonsmokers and smokers. *Am J Respir Crit Care Med* **187**,
500 1067-1075 (2013).
- 501 4. R. P. Dickson, J. R. Erb-Downward, C. M. Freeman, L. McCloskey, N. R. Falkowski, G. B. Huffnagle,
502 J. L. Curtis, Bacterial topography of the healthy human lower respiratory tract. *mBio* **8**, (2017).
- 503 5. A. A. Pragman, H. B. Kim, C. S. Reilly, C. Wendt, R. E. Isaacson, The lung microbiome in moderate
504 and severe chronic obstructive pulmonary disease. *PLoS One* **7**, e47305 (2012).
- 505 6. Y. J. Huang, E. Kim, M. J. Cox, E. L. Brodie, R. Brown, J. P. Wiener-Kronish, S. V. Lynch, A persistent
506 and diverse airway microbiota present during chronic obstructive pulmonary disease exacerbations.
507 *OMICS* **14**, 9-59 (2010).
- 508 7. M. M. Tunney, T. R. Field, T. F. Moriarty, S. Patrick, G. Doering, M. S. Muhlebach, M. C. Wolfgang,
509 R. Boucher, D. F. Gilpin, A. McDowell, J. S. Elborn, Detection of anaerobic bacteria in high numbers
510 in sputum from patients with cystic fibrosis. *Am J Respir Crit Care Med* **177**, 995-1001 (2008).
- 511 8. G. B. Rogers, C. J. van der Gast, L. Cuthbertson, S. K. Thomson, K. D. Bruce, M. L. Martin, D. J.
512 Serisier, Clinical measures of disease in adult non-CF bronchiectasis correlate with airway microbiota
513 composition. *Thorax* **68**, 731-737 (2013).
- 514 9. J. G. Bartlett, The role of anaerobic bacteria in lung abscess. *Clin Infect Dis* **40**, 923-925 (2005).
- 515 10. S. K. Lucas, R. Yang, J. M. Dunitz, H. C. Boyer, R. C. Hunter, 16S rRNA gene sequencing reveals
516 site-specific signatures of the upper and lower airways of cystic fibrosis patients. *J Cyst Fibros* **17**,
517 204-212 (2018).
- 518 11. P. L. Molyneaux, S. A. G. Willis-Owen, M. J. Cox, P. James, S. Cowman, M. Loebinger, A. Blanchard,
519 L. M. Edwards, C. Stock, C. Daccord, E. A. Renzoni, A. U. Wells, M. F. Moffatt, W. O. C. Cookson, T.
520 M. Maher, Host-microbial interactions in idiopathic pulmonary fibrosis. *Am J Respir Crit Care Med* **195**,
521 1640-1650 (2017).
- 522 12. L. N. Segal, J. C. Clemente, Y. Li, C. Ruan, J. Cao, M. Danckers, A. Morris, S. Tapyrik, B. G. Wu, P.
523 Diaz, G. Calligaro, R. Dawson, R. N. van Zyl-Smit, K. Dheda, W. N. Rom, M. D. Weiden, Anaerobic

- 524 bacterial fermentation products increase tuberculosis risk in antiretroviral-drug-treated HIV patients.
525 *Cell Host Microbe* **21**, 530-537.e534 (2017).
- 526 13. E. T. Zemanick, B. D. Wagner, S. D. Sagel, M. J. Stevens, F. J. Accurso, J. K. Harris, Reliability of
527 quantitative real-time PCR for bacterial detection in cystic fibrosis airway specimens. *PLoS One* **5**,
528 e15101 (2010).
- 529 14. I. Sulaiman, B. G. Wu, Y. Li, A. S. Scott, P. Malecha, B. Scaglione, J. Wang, A. Basavaraj, S. Chung,
530 K. Bantis, J. Carpenito, J. C. Clemente, N. Shen, J. Bessich, S. Rafeq, G. Michaud, J. Donington, C.
531 Naidoo, G. Theron, G. Schattner, S. Garofano, R. Condos, D. Kamelhar, D. Addrizzo-Harris, L. N.
532 Segal, Evaluation of the airway microbiome in nontuberculous mycobacteria disease. *Eur Respir J* **52**,
533 (2018).
- 534 15. B. Mirković, M. A. Murray, G. M. Lavelle, K. Molloy, A. A. Azim, C. Gunaratnam, F. Healy, D. Slattery,
535 P. McNally, J. Hatch, M. Wolfgang, M. M. Tunney, M. S. Muhlebach, R. Devery, C. M. Greene, N. G.
536 McElvaney, The role of short-chain fatty acids, produced by anaerobic bacteria, in the cystic fibrosis
537 airway. *Am J Respir Crit Care Med* **192**, 1314-1324 (2015).
- 538 16. P. Ghorbani, P. Santhakumar, Q. Hu, P. Djadeu, T. M. Wolever, N. Palaniyar, H. Grasemann, Short-
539 chain fatty acids affect cystic fibrosis airway inflammation and bacterial growth. *Eur Respir J* **46**, 1033-
540 1045 (2015).
- 541 17. J. M. Flynn, D. Niccum, J. M. Dunitz, R. C. Hunter, Evidence and role for bacterial mucin degradation
542 in cystic fibrosis airway disease. *PLoS Pathog* **12**, e1005846 (2016).
- 543 18. J. M. Flynn, L. C. Cameron, T. D. Wigger, J. M. Dunitz, W. R. Harcombe, R. C. Hunter, Disruption of
544 cross-feeding inhibits pathogen growth in the sputa of patients with cystic fibrosis. *mSphere* **5**, (2020).
- 545 19. L. A. Carmody, L. J. Caverly, B. K. Foster, M. A. M. Rogers, L. M. Kalikin, R. H. Simon, D. R.
546 VanDevanter, J. J. LiPuma, Fluctuations in airway bacterial communities associated with clinical states
547 and disease stages in cystic fibrosis. *PLoS One* **13**, e0194060 (2018).
- 548 20. M. R. Hendricks, L. P. Lashua, D. K. Fischer, B. A. Flitter, K. M. Eichinger, J. E. Durbin, S. N. Sarkar,
549 C. B. Coyne, K. M. Empey, J. M. Bomberger, Respiratory syncytial virus infection enhances
550 *Pseudomonas aeruginosa* biofilm growth through dysregulation of nutritional immunity. *Proc Natl Acad*
551 *Sci U S A* **113**, 1642-1647 (2016).
- 552 21. M. R. Kiedrowski, J. R. Gaston, B. R. Kocak, S. L. Coburn, S. Lee, J. M. Pilewski, M. M. Myerburg, J.
553 M. Bomberger, Biofilm growth on cystic fibrosis airway epithelial cells is enhanced during respiratory
554 syncytial virus coinfection. *mSphere* **3**, (2018).
- 555 22. S. Moreau-Marquis, J. M. Bomberger, G. G. Anderson, A. Swiatecka-Urban, S. Ye, G. A. O'Toole, B.
556 A. Stanton, The DeltaF508-CFTR mutation results in increased biofilm formation by *Pseudomonas*
557 *aeruginosa* by increasing iron availability. *Am J Physiol Lung Cell Mol Physiol* **295**, L25-37 (2008).

- 558 23 T. Fofanova, C. Stewart, J. Auchtung, R. Wilson, R. Britton, K. Grande-Allen, M. Estes, J. Petrosino,
559 A novel human enteroid-anaerobe co-culture system to study microbial-host interaction under
560 physiological hypoxia. *bioRxiv* **555755** (2019).
- 561 24. C. Evert, T. Loesekann, G. Bhat, A. Shajahan, R. Sonon, P. Azadi, R. C. Hunter, Generation of ¹³C-
562 labeled MUC5AC mucin oligosaccharides for stable isotope probing of host-associated microbial
563 communities. *ACS Infect Dis* **5**, 385-393 (2019).
- 564 25. M. Tamm, M. Bihl, O. Eickelberg, P. Stulz, A. P. Perruchoud, M. Roth, Hypoxia-induced interleukin-6
565 and interleukin-8 production is mediated by platelet-activating factor and platelet-derived growth factor
566 in primary human lung cells. *Am J Respir Cell Mol Biol* **19**, 653-661 (1998).
- 567 26. L. Jia, Y. Shi, Y. Wen, W. Li, J. Feng, C. Chen, The roles of TNFAIP2 in cancers and infectious
568 diseases. *J Cell Mol Med* **22**, 5188-5195 (2018).
- 569 27. K. De Filippo, A. Dudeck, M. Hasenberg, E. Nye, N. van Rooijen, K. Hartmann, M. Gunzer, A. Roers,
570 N. Hogg, Mast cell and macrophage chemokines CXCL1/CXCL2 control the early stage of neutrophil
571 recruitment during tissue inflammation. *Blood* **121**, 4930-4937 (2013).
- 572 28. E. K. Koltsova, K. Ley, The mysterious ways of the chemokine CXCL5. *Immunity* **33**, 7-9 (2010).
- 573 29. E. M. Peterman, C. Sullivan, M. F. Goody, I. Rodriguez-Nunez, J. A. Yoder, C. H. Kim, Neutralization
574 of mitochondrial superoxide by superoxide dismutase 2 promotes bacterial clearance and regulates
575 phagocyte numbers in zebrafish. *Infect Immun* **83**, 430-440 (2015).
- 576 30. J. M. Sallenave, G. A. Cunningham, R. M. James, G. McLachlan, C. Haslett, Regulation of pulmonary
577 and systemic bacterial lipopolysaccharide responses in transgenic mice expressing human elafin.
578 *Infect Immun* **71**, 3766-3774 (2003).
- 579 31. A. G. Henderson, C. Ehre, B. Button, L. H. Abdullah, L. H. Cai, M. W. Leigh, G. C. DeMaria, H. Matsui,
580 S. H. Donaldson, C. W. Davis, J. K. Sheehan, R. C. Boucher, M. Kesimer, Cystic fibrosis airway
581 secretions exhibit mucin hyperconcentration and increased osmotic pressure. *J Clin Invest* **124**, 3047-
582 3060 (2014).
- 583 32. D. J. Thornton, J. R. Davies, S. Kirkham, A. Gautrey, N. Khan, P. S. Richardson, J. K. Sheehan,
584 Identification of a nonmucin glycoprotein (gp-340) from a purified respiratory mucin preparation:
585 evidence for an association involving the MUC5B mucin. *Glycobiology* **11**, 969-977 (2001).
- 586 33. M. Audry, C. Robbe-Masselot, J. P. Barnier, B. Gachet, B. Saubaméa, A. Schmitt, S. Schönherr-
587 Hellec, R. Léonard, X. Nassif, M. Coureuil, Airway mucus restricts neisseria meningitidis away from
588 nasopharyngeal epithelial cells and protects the mucosa from inflammation. *mSphere* **4**, (2019).
- 589 34. S. Vishwanath, R. Ramphal, Adherence of *Pseudomonas aeruginosa* to human tracheobronchial
590 mucin. *Infect Immun* **45**, 197-202 (1984).
- 591 35. J. Y. Co, G. Cárcamo-Oyarce, N. Billings, K. M. Wheeler, S. C. Grindy, N. Holten-Andersen, K.
592 Ribbeck, Mucins trigger dispersal of. *NPJ Biofilms Microbiomes* **4**, 23 (2018).

- 593 36. M. Ulrich, I. Beer, P. Braitmaier, M. Dierkes, F. Kummer, B. Krismer, U. Schumacher, U. Gräpler-
594 Mainka, J. Riethmüller, P. Ø. Jensen, T. Bjarnsholt, N. Høiby, G. Bellon, G. Döring, Relative
595 contribution of *Prevotella intermedia* and *Pseudomonas aeruginosa* to lung pathology in airways of
596 patients with cystic fibrosis. *Thorax* **65**, 978-984 (2010).
- 597 37. E. T. Zemanick, B. D. Wagner, C. E. Robertson, R. C. Ahrens, J. F. Chmiel, J. P. Clancy, R. L. Gibson,
598 W. T. Harris, G. Kurland, T. A. Laguna, S. A. McColley, K. McCoy, G. Retsch-Bogart, K. T. Sobush,
599 P. L. Zeitlin, M. J. Stevens, F. J. Accurso, S. D. Sagel, J. K. Harris, Airway microbiota across age and
600 disease spectrum in cystic fibrosis. *Eur Respir J* **50**, (2017).
- 601 38. R. A. Quinn, K. Whiteson, Y. W. Lim, P. Salamon, B. Bailey, S. Mienardi, S. E. Sanchez, D. Blake, D.
602 Conrad, F. Rohwer, A Winogradsky-based culture system shows an association between microbial
603 fermentation and cystic fibrosis exacerbation. *ISME J* **9**, 1052 (2015).
- 604 39. R. Raghuvanshi, K. Vasco, Y. Vázquez-Baeza, L. Jiang, J. T. Morton, D. Li, A. Gonzalez, L. DeRight
605 Goldasich, G. Humphrey, G. Ackermann, A. D. Swafford, D. Conrad, R. Knight, P. C. Dorrestein, R.
606 A. Quinn, High-resolution longitudinal dynamics of the cystic fibrosis sputum microbiome and
607 metabolome through antibiotic therapy. *mSystems* **5**, (2020).
- 608 40. E. Jubinville, M. Veillette, J. Milot, F. Maltais, A. M. Comeau, R. C. Levesque, C. Duchaine,
609 Exacerbation induces a microbiota shift in sputa of COPD patients. *PLoS One* **13**, e0194355 (2018).
- 610 41. K. Yamasaki, H. Mukae, T. Kawanami, K. Fukuda, S. Noguchi, K. Akata, K. Naito, K. Oda, T. Ogoshi,
611 C. Nishida, T. Orihashi, Y. Kawanami, H. Ishimoto, H. Taniguchi, K. Yatera, Possible role of anaerobes
612 in the pathogenesis of nontuberculous mycobacterial infection. *Respirology* **20**, 758-765 (2015).
- 613 42. A. Venkataraman, M. A. Rosenbaum, J. J. Werner, S. C. Winans, L. T. Angenent, Metabolite transfer
614 with the fermentation product 2,3-butanediol enhances virulence by *Pseudomonas aeruginosa*. *ISME*
615 *J* **8**, 1210-1220 (2014).
- 616 43. J. Phan, T. Gallagher, A. Oliver, W. E. England, K. Whiteson, Fermentation products in the cystic
617 fibrosis airways induce aggregation and dormancy-associated expression profiles in a CF clinical
618 isolate of *Pseudomonas aeruginosa*. *FEMS Microbiol Lett* **365**, (2018).
- 619 44. J. Z. H. von Martels, M. Sadaghian Sadabad, A. R. Bourgonje, T. Blokzijl, G. Dijkstra, K. N. Faber, H.
620 J. M. Harmsen, The role of gut microbiota in health and disease: In vitro modeling of host-microbe
621 interactions at the aerobe-anaerobe interphase of the human gut. *Anaerobe* **44**, 3-12 (2017).
- 622 45. G.-S. Park, M. H. Park, W. Shin, C. Zhao, S. Sheikh, S. J. Oh, H. J. Kim, Emulating host-microbiome
623 ecosystem of human gastrointestinal tract *in vitro*. *Stem Cell Reviews and Reports* **13**, 321-334 (2017).
- 624 46. M. Yee, S. Kim, P. Sethi, N. Düzgüneş, K. Konopka, *Porphyromonas gingivalis* stimulates IL-6 and IL-
625 8 secretion in GSM-K, HSC-3 and H413 oral epithelial cells. *Anaerobe* **28**, 62-67 (2014).
- 626 47. A. Pinnock, C. Murdoch, K. Moharamzadeh, S. Whawell, C. W. I. Douglas, Characterisation and
627 optimisation of organotypic oral mucosal models to study *Porphyromonas gingivalis* invasion.
628 *Microbes and Infection* **16**, 310-319 (2014).

- 629 48. Y. W. Han, W. Shi, G. T. Huang, S. Kinder Haake, N. H. Park, H. Kuramitsu, R. J. Genco, Interactions
630 between periodontal bacteria and human oral epithelial cells: *Fusobacterium nucleatum* adheres to
631 and invades epithelial cells. *Infection and immunity* **68**, 3140-3146 (2000).
- 632 49. U. K. Gursoy, E. Könönen, V. J. Uitto, Prevotella intermedia ATCC 25611 targets host cell lamellipodia
633 in epithelial cell adhesion and invasion. *Oral Microbiology and Immunology* **24**, 304-309 (2009).
- 634 50. D. Ulluwishewa, R. C. Anderson, W. Young, W. C. McNabb, P. van Baarlen, P. J. Moughan, J. M.
635 Wells, N. C. Roy, Live *Faecalibacterium prausnitzii* in an apical anaerobic model of the intestinal
636 epithelial barrier. *Cellular Microbiology* **17**, 226-240 (2015).
- 637 51. A. Pinnock, C. Murdoch, K. Moharamzadeh, S. Whawell, C. W. Douglas, Characterisation and
638 optimisation of organotypic oral mucosal models to study *Porphyromonas gingivalis* invasion.
639 *Microbes Infect* **16**, 310-319 (2014).
- 640 52. W. Shin, A. Wu, M. W. Massidda, C. Foster, N. Thomas, D.-W. Lee, H. Koh, Y. Ju, J. Kim, H. J. Kim,
641 A robust longitudinal co-culture of obligate anaerobic gut microbiome with human intestinal epithelium
642 in an anoxic-oxic interface-on-a-chip. *Frontiers in Bioengineering and Biotechnology* **7**, 13 (2019).
- 643 53. M. Marzorati, B. Vanhoecke, T. De Ryck, M. Sadaghian Sadabad, I. Pinheiro, S. Possemiers, P. Van
644 den Abbeele, L. Derycke, M. Bracke, J. Pieters, T. Hennebel, H. J. Harmsen, W. Verstraete, T. Van
645 de Wiele, The HMI™ module: a new tool to study the host-microbiota interaction in the human
646 gastrointestinal tract in vitro. *BMC Microbiol* **14**, 133 (2014).
- 647 54. H. J. Kim, D. Huh, G. Hamilton, D. E. Ingber, Human gut-on-a-chip inhabited by microbial flora that
648 experiences intestinal peristalsis-like motions and flow. *Lab Chip* **12**, 2165-2174 (2012).
- 649 55. H. J. Kim, H. Li, J. J. Collins, D. E. Ingber, Contributions of microbiome and mechanical deformation
650 to intestinal bacterial overgrowth and inflammation in a human gut-on-a-chip. *Proc Natl Acad Sci U S*
651 *A* **113**, E7-15 (2016).
- 652 56. P. Shah, J. V. Fritz, E. Glaab, M. S. Desai, K. Greenhalgh, A. Frachet, M. Niegowska, M. Estes, C.
653 Jäger, C. Seguin-Devaux, F. Zenhausem, P. Wilmes, A microfluidics-based *in vitro* model of the
654 gastrointestinal human-microbe interface. *Nat Commun* **7**, 11535 (2016).
- 655 57. V. V. Thacker, N. Dhar, K. Sharma, R. Barrile, K. Karalis, J. D. McKinney, A lung-on-chip infection
656 model reveals protective and permissive roles of alveolar epithelial cells in tuberculosis. *bioRxiv*,
657 2020.02.03.931170 (2020).
- 658 58. G. G. Einarsson, D. M. Comer, L. McIlreavey, J. Parkhill, M. Ennis, M. M. Tunney, J. S. Elborn,
659 Community dynamics and the lower airway microbiota in stable chronic obstructive pulmonary
660 disease, smokers and healthy non-smokers. *Thorax* **71**, 795 (2016).
- 661 59. D. Papazian, T. Chhoden, M. Arge, T. Vorup-Jensen, C. H. Nielsen, K. Lund, P. A. Würtzen, S.
662 Hansen, Effect of polarization on airway epithelial conditioning of monocyte-derived dendritic cells. *Am*
663 *J Respir Cell Mol Biol* **53**, 368-377 (2015).

- 664 60. C. E. Stewart, E. E. Torr, N. H. Mohd Jamili, C. Bosquillon, I. Sayers, Evaluation of differentiated
665 human bronchial epithelial cell culture systems for asthma research. *J Allergy (Cairo)* **2012**, 943982
666 (2012).
- 667 61. C. I. Grainger, L. L. Greenwell, D. J. Lockley, G. P. Martin, B. Forbes, Culture of Calu-3 cells at the air
668 interface provides a representative model of the airway epithelial barrier. *Pharm Res* **23**, 1482-1490
669 (2006).
- 670 62. W. E. Finkbeiner, S. D. Carrier, C. E. Teresi, Reverse transcription-polymerase chain reaction (RT-
671 PCR) phenotypic analysis of cell cultures of human tracheal epithelium, tracheobronchial glands, and
672 lung carcinomas. *Am J Respir Cell Mol Biol* **9**, 547-556 (1993).
- 673 63. P. LeSimple, J. Goepf, M. L. Palmer, S. C. Fahrenkrug, S. M. O'Grady, P. Ferraro, R. Robert, J. W.
674 Hanrahan, Cystic fibrosis transmembrane conductance regulator is expressed in mucin granules from
675 Calu-3 and primary human airway epithelial cells. *Am J Respir Cell Mol Biol* **49**, 511-516 (2013).
- 676 64. D. Worlitzsch, R. Tarran, M. Ulrich, U. Schwab, A. Cekici, K. C. Meyer, P. Birrer, G. Bellon, J. Berger,
677 T. Weiss, K. Botzenhart, J. R. Yankaskas, S. Randell, R. C. Boucher, G. Döring, Effects of reduced
678 mucus oxygen concentration in airway *Pseudomonas infections* of cystic fibrosis patients. *J Clin Invest*
679 **109**, 317-325 (2002).
- 680 65. P. K. Singh, A. L. Schaefer, M. R. Parsek, T. O. Moninger, M. J. Welsh, E. P. Greenberg, Quorum-
681 sensing signals indicate that cystic fibrosis lungs are infected with bacterial biofilms. *Nature* **407**, 762-
682 764 (2000).
- 683 66. K. Martens, P. W. Hellings, B. Steelant, Calu-3 epithelial cells exhibit different immune and epithelial
684 barrier responses from freshly isolated primary nasal epithelial cells in vitro. *Clin Transl Allergy* **8**, 40
685 (2018).
- 686 67. Y. Liao, G. K. Smyth, W. Shi, The R package Rsubread is easier, faster, cheaper and better for
687 alignment and quantification of RNA sequencing reads. *Nucleic Acids Res* **47**, e47 (2019).
- 688 68. M. I. Love, W. Huber, S. Anders, Moderated estimation of fold change and dispersion for RNA-seq
689 data with DESeq2. *Genome Biol* **15**, 550 (2014).
- 690 69. M. Stephens, False discovery rates: a new deal. *Biostatistics* **18**, 275-294 (2017).

691

692

693 **ACKNOWLEDGEMENTS**

694 We thank the University of Minnesota Fabrication Shop for the custom design of our anaerobic chamber
695 culture manifold. **Funding.** This work was supported by the National Heart Lung and Blood Institute
696 (HL136919), a Cystic Fibrosis Postdoctoral Fellowship to P.J.M. (MOORE20F0), a National Institutes of
697 Health fellowship (#T90DE0227232) awarded through the National Institute of Dental and Craniofacial
698 Research to S.K.L., and an American Society for Microbiology Undergraduate Research Fellowship to
699 L.A.K. **Author contributions.** P.J.M. and R.C.H. were responsible for study design and wrote the
700 manuscript. P.J.M. T.D.W., L.A.K., S.J.A., S.K.L., and R.C.H., collected and analyzed the data and edited
701 the manuscript. T.D.W., S.J.A., and S.K.L. processed and analyzed RNA sequencing data. S.M.O.
702 contributed cell lines and assisted with experiments. **Competing interests.** The authors declare they have
703 no competing interests. **Data and materials availability.** All data needed to evaluate the conclusions are
704 present in the paper, Supplementary Materials, or available online at [https://github.com/Hunter-Lab-](https://github.com/Hunter-Lab-UMN/Moore_PJ_2020)
705 [UMN/Moore_PJ_2020](https://github.com/Hunter-Lab-UMN/Moore_PJ_2020).